

Investigation of Capability of Current Control by Electron Cyclotron Waves in the Quasi-axisymmetric Stellarator CFQS*

Yasuo YOSHIMURA¹⁾, Motonari KANDA¹⁾, Ryoma YANAI¹⁾, Akihiro SHIMIZU^{1,2)}, Shigeyoshi KINOSHITA¹⁾, Mitsutaka ISOBE^{1,2)}, Shoichi OKAMURA¹⁾, Kunihiro OGAWA^{1,2)}, Hiromi TAKAHASHI^{1,2)}, Takanori MURASE¹⁾, Sho NAKAGAWA¹⁾, Hiroyuki TANOUE¹⁾, Haifeng LIU³⁾ and Yuhong XU³⁾

¹⁾National Institute for Fusion Science, National Institutes of Natural Sciences, Toki, Gifu 509-5292, Japan

²⁾The Graduate University for Advanced Studies, SOKENDAI, Toki, Gifu 509-5929, Japan

³⁾Institute of Fusion Science, School of Physical Science and Technology, Southwest Jiaotong University, Chengdu, China

(Received 9 January 2022 / Accepted 3 March 2022)

The capability of plasma current control by the second harmonic electron cyclotron current drive in the quasi-axisymmetric stellarator CFQS is investigated. We used the ray-tracing code TRAVIS to evaluate the electron cyclotron (EC) wave power deposition and driven current. In the standard magnetic field configuration of CFQS, the poloidal distribution of the magnetic field is nearly axisymmetric, i.e., equivalent at all toroidal positions as tokamaks. In the calculation, a flat electron density profile at the core region with $n_{e0} = 1 \times 10^{19} \text{ m}^{-3}$ and a center-peaked electron temperature profile with $T_{e0} = 3.5 \text{ keV}$ are assumed. The EC wave beam direction is scanned mainly in the toroidal direction, aiming at the plasma axis. The vertical injection angle of the beam and magnetic field strength are varied and optimized to keep on-axis power deposition to maximize driven current at each toroidal direction of the EC wave beam. According to the calculation, the maximum driven current at optimum beam direction, with an expected maximum EC wave power of 400 kW, is approximately 80 kA. Meanwhile, approximately 26 kA of bootstrap current in CFQS with the volume-averaged β value of 1.2% is estimated using the BOOTSJ code. Hence, sufficient on-axis EC-driven current can be expected for compensation of the possible bootstrap current, although the current profiles are different. Moreover, a driven current of over 30 kA can be expected even in extreme cases where the magnetic field on-axis has ripples by modified modular coil currents by 20%. The possibility of compensation of bootstrap current in total amount and current profile is also discussed.

© 2022 The Japan Society of Plasma Science and Nuclear Fusion Research

Keywords: electron cyclotron current drive, ECCD, quasi-axisymmetric stellarator, CFQS

DOI: 10.1585/pfr.17.2402039

1. Introduction

A quasi-axisymmetric (QAS) stellarator CFQS [1] is under construction on a campus of Southwest Jiaotong University (SWJTU), China, as a joint project between SWJTU and National Institute for Fusion Science (NIFS), Japan. The project aims to prove the concept and advantages of QAS as a plasma confinement device. The CFQS will be the world's first realized QAS device. Because of the QAS configuration generated by external coils, favorable plasma confinement as tokamaks from the viewpoint of neoclassical theory and stable plasma sustainment as stellarators will be simultaneously performed. Specific parameters of the CFQS device are the major radius of 1 m, magnetic field strength of 1 T, aspect ratio of 4, and toroidal periodic number of 2. The magnetic field coil system consists of 16 (4 types \times 4 sections) modular coils

(Fig. 1), 12 toroidal field coils, and four poloidal field coils. As the heating devices for the CFQS, using a

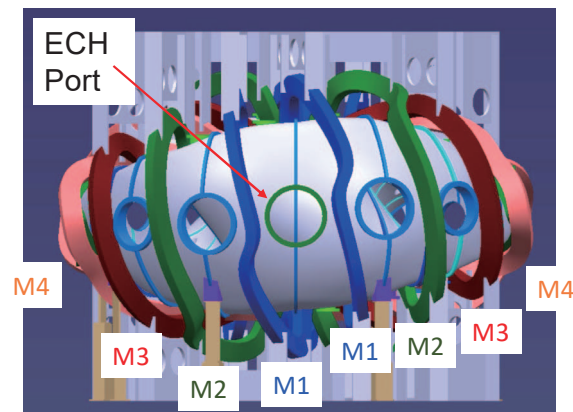


Fig. 1 Side view of the CFQS vacuum vessel with modular coils. A round port assigned for ECH power injection is seen at the center in this view.

author's e-mail: yoshimura.yasuo@nifs.ac.jp

*) This article is based on the presentation at the 30th International Toki Conference on Plasma and Fusion Research (ITC30).

54.5 GHz gyrotron (max. pulse length of 100 ms, max. output power of 450 kW) [2] for electron cyclotron heating and current drive (ECH and ECCD) and neutral beam injection system, which were formerly used for Compact Helical System (CHS) [3] experiments at NIFS, is planned.

Although QAS devices do not require plasma current, current control will be a beneficial tool for improving plasma confinement through the modification of profiles of plasma current and rotational transform or maintaining the designed magnetic configuration. Therefore, this study investigates the capability of current control by electron cyclotron (EC) waves in the CFQS device. The remainder of the paper is organized as follows. Section 2 describes the setup of the calculation using ray-tracing code. Section 3 presents calculation results. Finally, Section 4 presents the conclusion.

2. Setup of Calculation

The EC wave power injection system in CFQS is planned as follows. The power source will be a 54.5 GHz gyrotron, which has been used for CHS device in NIFS formerly. The EC wave generated by the gyrotron will be transmitted through a corrugated waveguide transmission line to the CFQS vacuum vessel and then injected into plasmas by the EC wave antenna system. Figure 2 shows the present design of the antenna. The antenna consists of four mirrors: two focusing mirrors, one fixed plane mirror, and one two-dimensional (2D) steerable plane mirror to control the EC wave beam direction. The center position of the steerable mirror is $(R, T, Z) = (1.694, 0, 0.085)$. Here R , T , and Z denote coordinates in a major radial direction, toroidal direction, and vertical direction, respectively. The beam is formed as a circular Gaussian profile focused at the plasma center with a 30 mm waist radius. The beam direction is defined by the parameters T_f and Z_f , describing the position of the beam center on a virtual plane target placed at $R = 1.2$ m. The positive direction of T and T_f is a right side looking from the outside of the device.

To evaluate EC-driven currents in CFQS, the ray-tracing code TRAVIS [4] is used with the flat electron density profile at the core region with $n_{e0} = 1 \times 10^{19} \text{ m}^{-3}$ and center-peaked electron temperature profile with $T_{e0} = 3.5 \text{ keV}$, as shown in Fig. 3. The injected EC wave power is set to 400 kW in extraordinary mode. This plasma parameter set would be achievable in CFQS though it is at the slightly outer edge of CHS plasma parameter space, because of the improved confinement which will be realized in CFQS than that of CHS.

Applying the parameters of the EC wave beam and plasma described above, scanning the beam direction mainly in toroidal direction T_f with adjusting the beam direction in vertical direction Z_f to follow the vertical displacement of the magnetic axis, and adjusting the magnetic field to assure the Doppler-shifted on-axis resonance condition, on-axis EC-driven currents are calculated in three

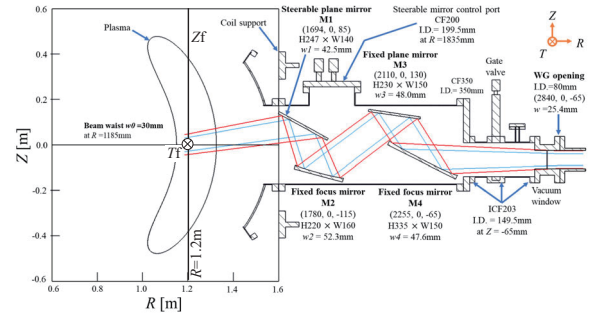


Fig. 2 Present design of EC wave beam injection antenna system consisting of four mirrors. The EC wave is transmitted through corrugated waveguide transmission line and injected into plasmas as a circularly focused Gaussian beam. In this figure, the beam direction setting parameters T_f and Z_f are set as 0 m.

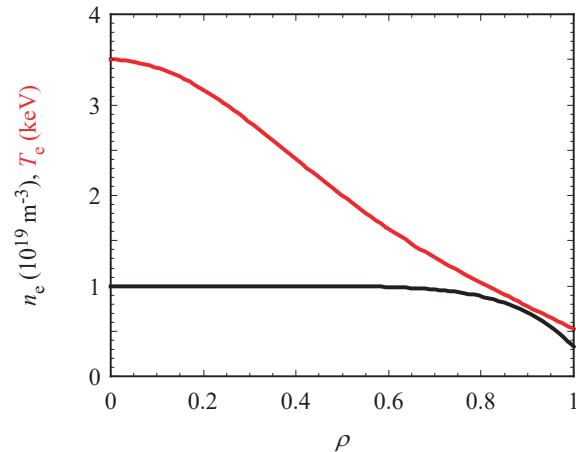


Fig. 3 Electron density (black) and temperature (red) profiles assumed in the TRAVIS calculation. $n_{e0} = 1 \times 10^{19} \text{ m}^{-3}$ and $T_{e0} = 3.5 \text{ keV}$.

types of magnetic configurations of CFQS.

3. Results of the Driven Current Calculation

3.1 Standard magnetic configuration

First, a typical magnetic field configuration of CFQS, standard (STD) configuration, is investigated. In the STD configuration, the coil currents in all four types of modular coils, M1, M2, M3, and M4 (Fig. 1), are equivalent, and the poloidal distribution of magnetic field strength is nearly constant in toroidal direction, that is, quasisymmetric as shown in Fig. 4 (a) for magnetic axis. The EC wave injection is assigned at a port allocated at the toroidal angle φ of 90° . Toroidal current is driven by toroidally oblique injection of EC wave beam characterized with the toroidal beam direction parameter T_f . In the TRAVIS calculations of EC-driven current, T_f is scanned, adjusting magnetic field strength represented by the on-axis strength at $\varphi = 90^\circ$, B_{90} , and Z_f to maintain on-axis heating condition

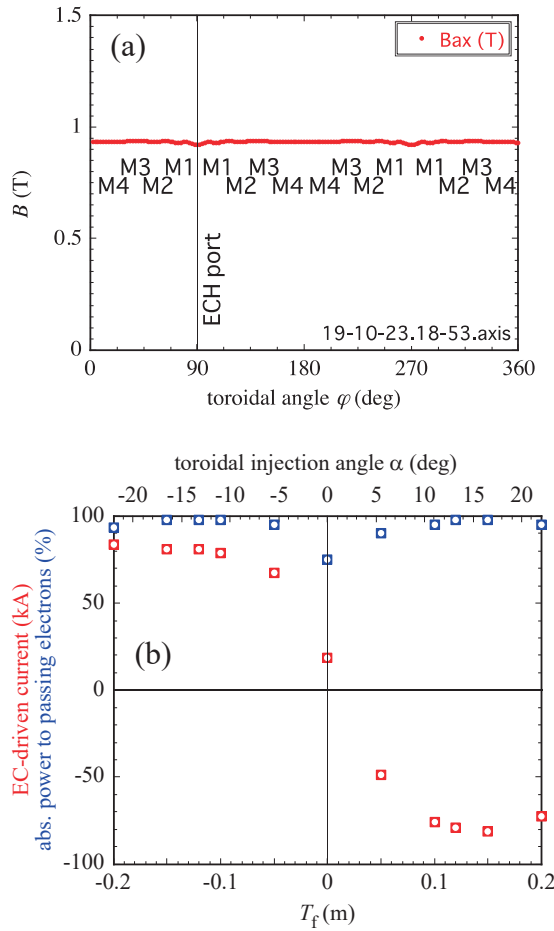


Fig. 4 (a) Toroidal distribution of the magnetic field on-axis in the STD configuration in the case of $B_{90} = 0.93$ T. (b) EC-driven currents (red open squares) and absorbed power ratios to passing electrons (blue open squares) in the STD configuration against toroidal beam direction parameter T_f and toroidal beam injection angle α .

and maximize driven current, for example, when $T_f = 0$ m, $B_{90} = 0.98$ T, and $Z_f = 0$ m, and when $T_f = +0.2$ m, $B_{90} = 0.9$ T, and $Z_f = 0.07$ m.

T_f is scanned in the range of -0.2 to $+0.2$ m, corresponding to the toroidal cross-sections at $\varphi = 76.4^\circ$ to 103.4° , where most wave powers are absorbed. Additionally, the range of $T_f = -0.2$ to $+0.2$ m corresponds to the range of -22° to $+22^\circ$ of beam injection angle α measured from the plane of $T = 0$ m. Figure 4 (b) shows the calculated results. The EC wave power absorption efficiency is almost 100%, and almost all power is absorbed by passing electrons regardless of T_f value, except for $T_f = 0$ m. However, for EC-driven current, with the variation of T_f from 0 m, the absolute value of the driven current increases to approximately 80 kA and then saturates at more than ± 0.1 m. Thus, if the injected EC wave power of 400 kW is assumed, the EC-driven current up to 80 kA can be expected. Here, the current is nonzero at $T_f = 0$ m because of the up-shifted beam start point (center position of the steerable plane mirror) and the three-dimensional magnetic

axis of CFQS. According to the BOOTSJ code [5], approximately 26 kA of bootstrap current in the CFQS STD configuration with the volume-averaged β value of approximately 1.2% is estimated [6]. The β of approximately 1.2% would be maximum with planned total heating power for CFQS. The β corresponds to $n_{e0} = 1 \times 10^{19} \text{ m}^{-3}$, $T_{e0} = 3.5$ keV, and $T_{i0} = 2.6$ keV. Then, sufficient on-axis EC-driven current can be expected for compensation of the possible bootstrap current, ignoring the matching of current profiles. Because of the pressure gradient-driven nature of bootstrap current, bootstrap current profile tends to be hollow, whereas ECCD is the most effective at the center of plasma volume.

By changing the sign of T_f , the co- and counter-ECCD or making the rotational transform increase and decrease, at the plasma core region will be available.

In the above discussion, $T_{e0} = 3.5$ keV is assumed. T_{e0} is one of the key parameters that determine the driven current. If T_{e0} is assumed to be 3, 2, and 1 keV with the same n_{e0} of $1 \times 10^{19} \text{ m}^{-3}$, the highest driven current varies as ~ 65 , ~ 35 , and ~ 10 kA, respectively. Then, the statement of the discussion is valid for a wide range of T_{e0} .

The capability of off-axis ECCD is also investigated. When EC wave beam direction is tilted vertically with $n_{e0} = 1 \times 10^{19} \text{ m}^{-3}$, $T_{e0} = 3.5$ keV, and $T_f = -0.15$ m, the peak position of the power deposition shifts to $\rho = 0.2$, 0.4, 0.6, and 0.8, and the driven current varies as ~ 60 , ~ 37 , ~ 18 , and ~ 9 kA, respectively, because of the decrease in electron temperature and the increase in magnetic ripple along the magnetic field lines. In all cases, the radial distributions of driven currents are peaked and localized as $\Delta\rho < 0.2$.

3.2 Coil currents +20% configuration

As an extreme case, ECCD property in a configuration with magnetic ripples by setting currents of coils M3 and M4 increase by +20% from the STD configuration is investigated. In this case, heating positions are nearly at the bottom of the magnetic ripple, as shown in Fig. 5 (a), so that the EC-driven current is reduced because of the mirror effect. The calculated results summarized in Fig. 5 (b) show that although the absorbed power ratio to passing electrons is not reduced so much, the EC-driven current in the +20% configuration reduced significantly by $\sim 60\%$. The mirror reflection caused by the ripple-bottom heating and reduced toroidal velocity of passing electrons contribute to the significant reduction of the EC-driven current. However, more than 30 kA of EC-driven current, which is larger than the bootstrap current in the STD configuration, will be generated by 400 kW injection power, even in the +20% configuration.

3.3 Coil currents -20% configuration

As another extreme case, -20% configuration with M3 and M4 coil currents reduced by 20% from the STD

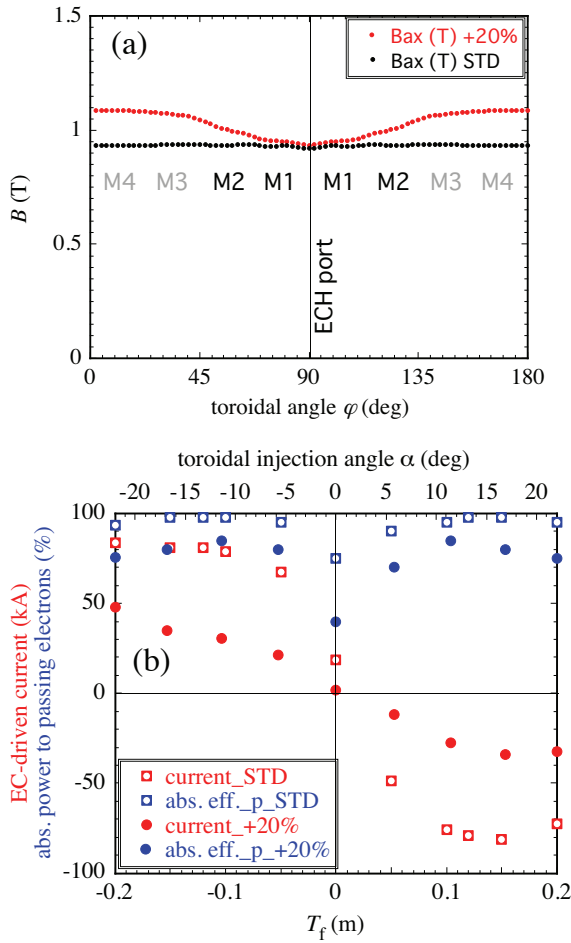


Fig. 5 (a) Example of the toroidal distribution of the magnetic field on-axis in the +20% configuration (red). (b) EC-driven currents (red closed circles) and absorbed power ratios to passing electrons (blue closed circles) in the +20% configuration. Data in the STD configuration are also plotted for comparison.

configuration is addressed. In this case, heating positions are nearly at the top of the magnetic ripple, as shown in Fig. 6(a). Near-ripple-top heating hardly affects the absorbed power ratio to passing electrons, and the property of ECCD is not degraded so much from that in the STD configuration; almost 80% of the driven current in the STD case can be driven in the -20% configuration, as shown in Fig. 6(b).

3.4 Discussion on the driven current distribution

All driven current calculations described above are performed with the designed EC wave beam characteristics; circular Gaussian profile focused at the plasma center with a 30 mm waist radius. The narrow power deposition due to the focused beam is advantageous for controlling localized power deposition and current drive and heat transport analysis. However, as described in Subsection 3.1, the driven current profile is too narrow to compensate for the expected wide profile of the bootstrap current [6], as

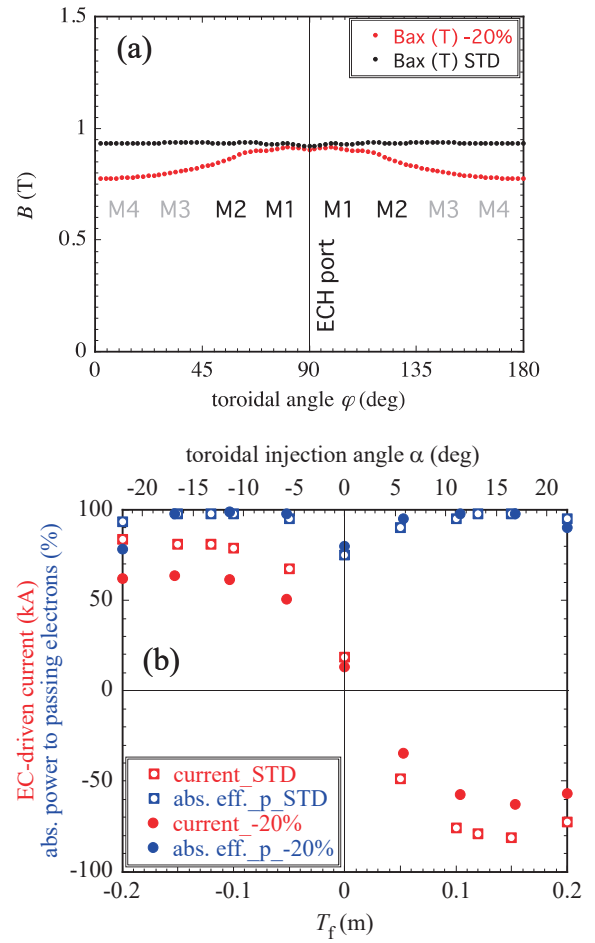


Fig. 6 (a) Example of the toroidal distribution of the magnetic field on-axis in the -20% configuration (red). (b) EC-driven currents (red closed circles) and absorbed power ratios to passing electrons (blue closed circles) in the -20% configuration. Data in the STD configuration are also plotted for comparison.

shown in Fig. 7(a). Here, the modification of the beam profile to widen the driven current profile is investigated by considering a 2D Gaussian beam with a 30 mm waist radius in the toroidal direction and a 160 mm radius in the vertical direction at the plasma center, aiming the beam direction to make the peak position of the driven current profile to be off-axis. The EC-driven current profile with the modified beam is plotted in red in Fig. 7(a), together with the EC-driven current profile with the focused on-axis beam in blue and the typical bootstrap current profile in black. All current profiles are normalized at each maximum value. In the modified beam case, the amount of driven current is 24.1 kA with the same plasma parameters shown in Fig. 3. Figure 7(b) shows the rotational transform profiles of CFQS standard configuration in vacuum (green), with the current of 24.1 kA driven by the modified EC wave beam (red), and with the bootstrap current assuming the amount of 24.1 kA (black). Here, the two kinds of currents are in opposite directions. A rotational transform

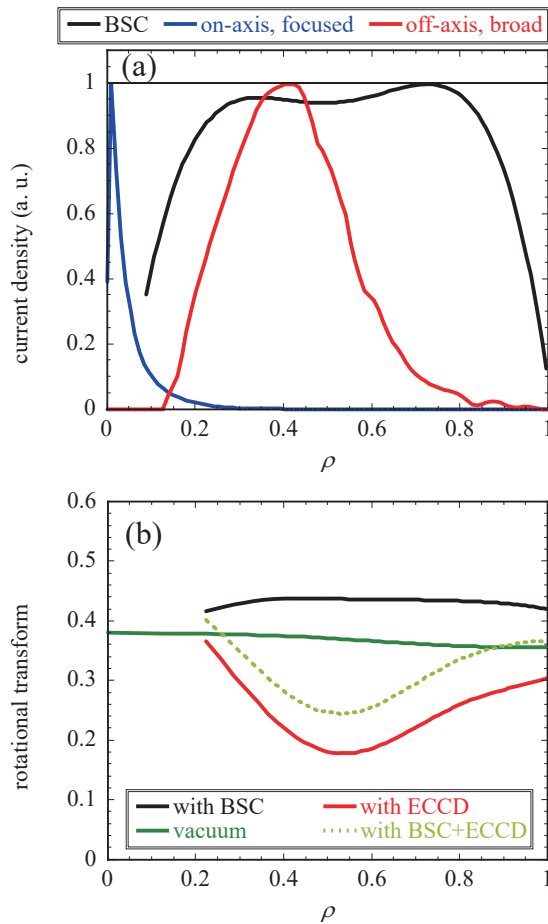


Fig. 7 (a) Normalized current density profiles in cases of bootstrap current (black), ECCD by on-axis focused beam (blue), and ECCD by off-axis broad beam (red). (b) Profiles of rotational transform in the cases of vacuum field (green), with bootstrap current (black), ECCD by off axis broad beam (red), and bootstrap current + ECCD (light green).

profile with the bootstrap and modified EC-driven currents is plotted in light green. Although the procedure of compensation for the bootstrap current profile by the modified EC wave beam is not optimized in this study, because of the center-peaked beam power profile and degradation of current drive efficiency at the outer plasma region, sufficient compensations of the bootstrap current profile and the resultant change in the rotational transform profile would be difficult in the Gaussian beam optic framework. To per-

form sufficient compensation, a more sophisticated design of EC wave beam power profile by a dedicated ECH system is essential.

4. Conclusions

For the physics basis of the CFQS project, the property of second harmonic ECCD using 54.5 GHz frequency and 400 kW power is investigated for plasma control, such as the control of plasma current, modification of rotational transform, and compensation of bootstrap current. According to the calculations by the ray-tracing code TRAVIS, where the flat electron density profile with $n_{e0} = 1 \times 10^{19} \text{ m}^{-3}$ and center-peaked electron temperature profile with $T_{e0} = 3.5 \text{ keV}$ are assumed, EC-driven currents larger than 30 kA can be expected in the standard QAS magnetic field configuration and even in the extreme configurations with $\pm 20\%$ magnetic ripples. The BOOTSJ code calculates approximately 26 kA of bootstrap current in the CFQS STD configuration with an expected maximum volume-averaged β value of approximately 1.2%. Thus, it is confirmed that at least as the absolute value, sufficient EC-driven current will be available in the CFQS various magnetic configurations to compensate for possible bootstrap current by the planned ECH system. Experimental investigations that require plasma current and rotational transform controls can be conducted. To make the driven current profile match with the bootstrap current profile, realizing a rather sophisticated EC wave beam power distribution by a dedicated ECH system will be required.

Acknowledgments

This research is supported by programs of international collaborations with overseas laboratories (UFEX105), promotion of magnetic confinement research using helical devices in Asia (URSX401), and the NIFS general collaboration project (NIFS18KBAP041, NIFS20KBAP067, and NIFS20KBAE001).

- [1] A. Shimizu *et al.*, Nucl. Fusion **62**, 016010 (2022).
- [2] Y. Yoshimura *et al.*, Plasma Fusion Res. **3**, S1076 (2008).
- [3] K. Matsuoka *et al.*, Plasma Phys. Control. Fusion **42**, 1145 (2000).
- [4] N.B. Marushchenko *et al.*, Phys. Plasmas **18**, 032501 (2011).
- [5] K.C. Shaing *et al.*, Phys. Fluids **B1**, 148 (1989).
- [6] A. Shimizu *et al.*, Plasma Fusion Res. **13**, 3403123 (2018).